関西電力株式会社
北海道電力株式会社
四国電力株式会社
九州電力株式会社
日本原子力発電株式会社

美浜 **2** 号機 　１次冷却材管実機材を使用した
熱時効脆化予測モデル（Ｈ３Ｔモデル）の妥当性

1. はじめに

本資料は、美浜２号機の１次冷却材管実機材（蒸気発生器取替工事（ＳＧＲ）時の切出し材）を使用して実施した過去の研究成果を用いて、熱時効脆化予測モデル（Ｈ３Ｔモデル）の妥当性を示すものである。

2. 試験状況

対象研究

美浜２号機 #14 SGR において切り出した SG 入口 50°エルボ（H/L エルボ材）、SG 出口 40°エルボ（CO/L エルボ材）を用いて以下の研究を実施している。

　① 電共研「２相ステンレス鋼の熱時効脆化度測定技術に関する研究」(平成７年３月)
　② 電共研「１次冷却材管等の時効劣化に関する研究(STEPⅢ)(その２)」(平成 11 年３月)

対象材料

研究①においては、切り出したままの材料（受入材）、研究②においては、切り出した材料に対してさらなる加速時効を実施した材料（追加時効材）をそれぞれ対象としている（表１、２及び図１参照）。
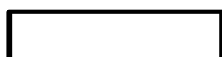
表1 対象材料の時効時間

研究	部位 (注1)	運転温度	実機時効時間 (注2)	追加時効時間 (時効温度)	時効時間合計
研究①	H/L エルボ材 (受入材)	約320℃	105,000 時間	—	105,000 時間
	CO/L エルボ材 (受入材)	約290℃	105,000 時間	—	105,000 時間
研究②	H/L エルボ材 (追加時効材)	約320℃	105,000 時間	5,000 時間(400℃) [46,700 時間(約320℃)相当]	151,700 時間 (注3)
			105,000 時間	10,000 時間(400℃) [93,400 時間(約320℃)相当]	198,400 時間 (注3)
	CO/L エルボ材 (追加時効材)	約290℃	105,000 時間	10,000 時間(400℃) [325,100 時間(約290℃)相当]	430,100 時間 (注3)

（注1） 材質は CF8M（JIS：SCS14A 相当）であり、静鋳造である。

（注2） 実機時効時間とは実運転時間である。

（注3） 追加時効時間を運転温度での時効時間に換算した相当時間である。

表2 対象材料の化学成分及びフェライト量

対象	Cr	Ni	Mo	N(注1)	Si	Nb(注1)	C	Mn	F%(注2)
H/L エルボ材 (M2HR1)									
CO/L エルボ材 (M2CR1)									

（注1） N と Nb は材料証明書に記載がないため、　　　　　　　　とする。

（注2） ASTM A800 により求めたフェライト量

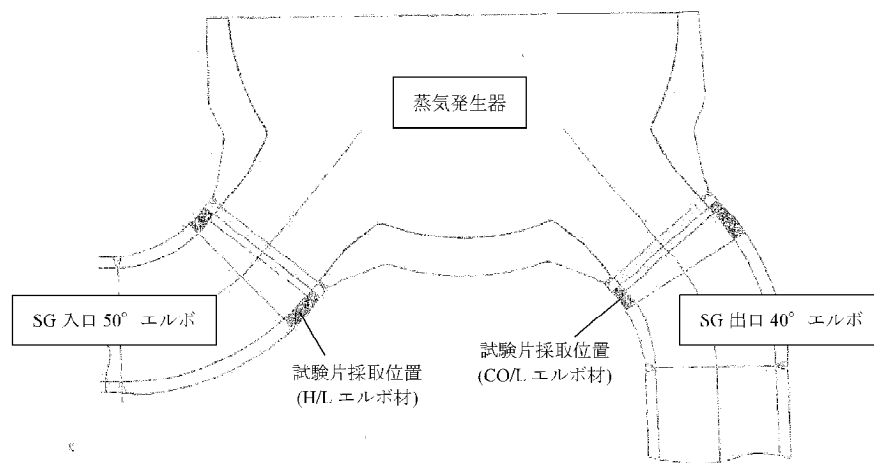
図1 試験片採取位置

　　　　　　　　　　の範囲は機密に係る事項ですので公開することはできません。

材料試験は機械試験として、引張試験、シャルピー衝撃試験、破壊靭性試験を、冶金試験として金相試験、硬さ試験を実施している。なお、研究②においては、破壊靭性等の確認に主眼を置いているため、引張試験ならびに金相試験は実施していない。

破壊靭性試験は以下の通り実施している。

 試験規格：ASTM E813-89
 試験方法：単一試験片を用いた除荷コンプライアンス法
 試 験 片：コンパクト試験片（１ＴＣＴ型）
     繰返低荷重による疲労亀裂ならびに片側 10%の側溝を有するもの、図２参照
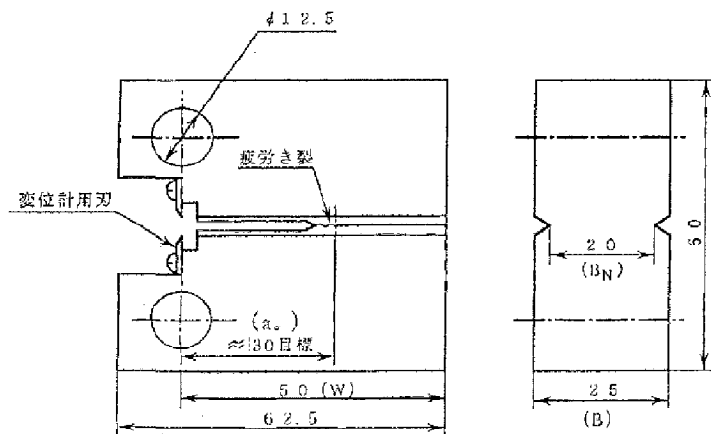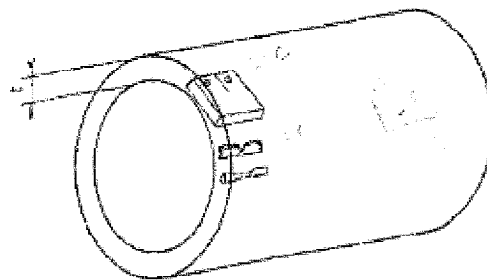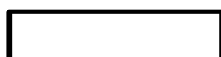   破面が管の周方向と同じ方向になるように採取した、図３参照
 試験条件：325℃、大気中

図２　試験片の形状及び寸法（１ＴＣＴ型）

図３　試験片の採取イメージ

破壊靭性試験の結果のうち、３項にてＨ３Ｔモデルとの比較を行った亀裂長さ 6mm における破壊靭性値(J_6)の結果は表３のとおりである。また、シャルピー衝撃試験結果及び引張試験結果を表４及び５に併せて示す。

   　　　　　　　　の範囲は機密に係る事項ですので公開することはできません。

表 3 破壊靭性試験結果

部位	運転温度	時効時間	$J_6 [kJ/m^2]$ (注)
H/L エルボ材	約 320℃	105,000 時間	
		151,700 時間	
		198,400 時間	
CO/L エルボ材	約 290℃	105,000 時間	
		430,100 時間	

（注） Δa=6mm における破壊靭性値、試験温度はすべて 325℃である。

　　　　　　　　　　の範囲は機密に係る事項ですので公開することはできません。

4
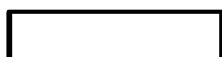
表4 シャルピー衝撃試験結果

部位	運転温度	時効時間	吸収エネルギ[注] [J]	横膨出量[注] [mm]
H/L エルボ材	約320℃	105,000 時間		
		151,700 時間		
		198,400 時間		
CO/L エルボ材	約290℃	105,000 時間		
		430,100 時間		

（注）試験温度はすべて 325℃である。

表5 引張試験結果

部位	運転温度	時効時間	0.2%耐力[注] [kgf/mm²]	引張強さ[注] [kgf/mm²]	伸び[注] [%]	絞り[注] [%]
H/L エルボ材	約320℃	105,000 時間				
		151,700 時間	-	-	-	-
		198,400 時間	-	-	-	-
CO/L エルボ材	約290℃	105,000 時間				
		430,100 時間	-	-	-	-

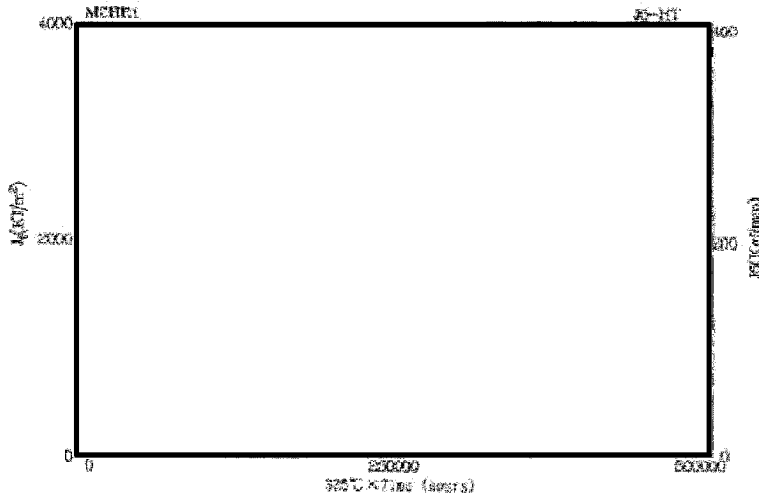（注）試験温度はすべて 325℃である。

<div style="border:1px solid black; display:inline-block">   </div> の範囲は機密に係る事項ですので公開することはできません。

3. 熱時効脆化予測モデル（Ｈ３Ｔモデル）と試験結果との比較

文献[1]に記載の予測モデル（Ｈ３Ｔモデル）に当該材料の材料証明書より表２に示す諸条件をインプットして求めた予測線と表３の破壊靭性試験の結果(J_6)をプロットした図を以下に示す。

Ｈ３Ｔモデル	予測式	
平均線	$J_6 =$	
下限線	$J_6 =$	

図4.2.4－2 J_6の変化（ホットレグ母材，試験温度 325℃）
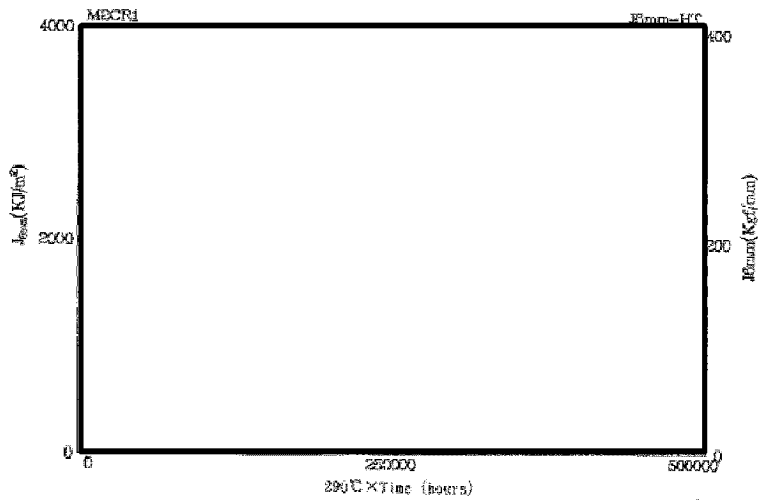
Ｈ３Ｔモデル	予測式	
平均線	$J_6 =$	
下限線	$J_6 =$	

図4.2.4－4 J_6の変化（クロスオーバレグ母材，試験温度 325℃）

図４ Ｈ３Ｔモデルの予測値と試験結果との比較

以上のとおり、受入材・追加時効材ともにＨ３Ｔモデルの予測値と比較した結果、予測下限線(-2σ)に包絡された結果となった。なお、ホットレグエルボ材は受入れの時点で靭性が底値になっていると考えられる。また、靭性値にばらつきが見られるが、試験片採取位置等のばらつきと考えられ、Ｈ３Ｔモデルはこのようなばらつきも考慮したモデルである。

□□□□□□□□ の範囲は機密に係る事項ですので公開することはできません。

6
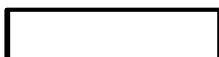
参考文献

[1] S.Kawaguchi et al., "Prediction Method of Tensile Properties and Fracture Toughness of Thermally Aged Cast Duplex Stainless Steel Piping," PVP2005-71528, 2005.（添付－１参照）

PVP2005-71528

PREDICTION METHOD OF TENSILE PROPERTIES AND FRACTURE TOUGHNESS OF THERMALLY AGED CAST DUPLEX STAINLESS STEEL PIPING

Seiichi KAWAGUCHI
Takasago R & D Center, Mitsubishi Heavy Industries Ltd.
Takasago Japan

Takeharu NAGASAKI   **Koji KOYAMA**
Kobe Shipyard & Machinery Works, Mitsubishi Heavy Industries Ltd.
Kobe Japan

ABSTRACT

Cast duplex stainless steels of CF8M and CF8 are used in major components because of their superior characteristics, such as corrosion resistance, weldability, and so on. However, these stainless steels are known to have tendency of thermal aging embrittlement after long term service. Therefore, the mechanical properties have been investigated using tensile test specimens and fracture toughness specimens aged at 300 to 450°C for up to 40,000 hours.

From the results, the effects of thermal aging on the mechanical properties of these cast duplex stainless steels were identified. The true stress-true strain curve prediction method (TSS model) and fracture toughness prediction method (H3T model) after long term service were established. These prediction methods are used for the evaluation on the plant life management of nuclear power plants in Japan.

NOMENCLATURE

CV : Charpy Absorbed Energy (J)
CVRT : Charpy Absorbed Energy at Room Temperature
CVHT : Charpy Absorbed Energy at High Temperature (325°C)
Δa : Stable Crack Extension
TSS model : True Stress-True Strain model
H3T model : Hyperbolic Time Temperature Toughness model
J_{Ic} : J Integral Value at the Initiation of Crack Extension
J_Q : J Integral Value at the Initiation of Crack Extension Defined in ASTM E813-89
J_6 : J Integral Value at Δa=6mm
F% : Ferrite Content
Creq : Chromium Equivalent
Nieq : Nickel Equivalent
P : Aging Parameter
R : Gas Constant
Q : Activation Energy

σ_y, σ_{y0} : 0.2% Proof Stress , Unaged 0.2% Proof Stress
σ_B : Tensile Strength
σ_f, σ_{f0} : Flow Stress , Unaged Flow Stress
ε_y : σ_y/E
E : Young's modulus
S : Standard Deviation
t_F : Initiation Time of Tertiary Embrittlement
APFIM : Atom Probe Field Ion Microscopy

1. INTRODUCTION

Cast duplex stainless steel, such as CF8M (SCS14A), CF8 (SCS13A), etc. is used for major components because of its excellent corrosion resistance, weldability, and so on. However, recent studies have reported that the mechanical properties of these cast duplex stainless steels have tendency of thermal aging embrittlement after long term service at relatively low temperatures between about 300 and 450°C[1, 2]. Therefore, it is necessary to comprehend the aging behavior of cast duplex stainless steel and contribute to the assessment of material degradation.

Seven kinds of cast duplex stainless steels of 70 to 140 mm in thickness were prepared in order to investigate the effect of the ferrite content on the thermal aging of cast duplex stainless steel. These test materials were long term heated at 300 to 450°C (up to 40,000 hours) and used for the tests[3,9,10]. Tensile tests, Charpy impact tests, and fracture toughness tests were carried out to investigate the mechanical property changes due to thermal aging. In addition, the microstructure changes were investigated[6,9,10].

At the same time as the above test programs, we also analyzed existing data, and developed the true stress-true strain curve prediction method (TSS model) and fracture toughness (J_{Ic}, J_6, J-Δa curve) prediction method (H3T model) for long term service[3,10,12].

Table 1   Chemical Composition

Reference	Material		Production method	Mark	Chemical composition (wt%)								Ferrite content* F%(%)
					C	Si	Mn	Ni	Cr	Mo	N	O	
This Study	Base metal	CF 8M (SCS14A)	Centrifugal casting	A-A	0.048	0.64	0.84	10.46	20.01	2.16	0.051	0.0075	10.3
				A-B	0.053	0.95	0.80	9.52	20.52	2.20	0.045	0.0078	17.4
				A-C	0.044	1.16	0.62	9.10	20.60	2.24	0.049	0.0058	23.1
				A-D	0.059	0.96	0.76	9.28	20.61	2.15	0.049	0.0118	17.4
				A-E	0.050	1.30	0.84	9.32	20.75	2.30	0.042	0.0129	23.0
		CF 8 (SCS13A)	Static casting	A-F	0.059	1.07	0.70	8.21	19.19	0.13	0.039	0.0072	9.5
				A-G	0.051	1.20	0.56	8.04	20.41	0.12	0.038	0.078	15.9
10) Suzuki	Base metal	CF 8M (SCS14A)	Centrifugal casting	B-A	0.050	1.51	0.90	10.30	21.30	3.10	0.060	0.004	22.5
				B-B	0.053	0.95	0.80	9.52	20.52	2.20	0.045	0.008	17.4
				B-C	0.048	0.64	0.84	10.46	20.01	2.16	0.051	0.008	10.3
			Static casting	B-E	0.076	1.12	0.44	9.20	19.80	2.10	0.027	0.003	16.5
				B-F	0.050	1.11	0.54	9.10	20.50	2.50	0.021	0.003	26.1
		CF 8 (SCS13A)		B-G	0.040	1.15	0.66	8.51	20.69	0.25	0.053	0.013	17.2
2) Chopra	Base metal	CF 8M (SCS14A)	Static casting	75	0.065	0.67	0.55	9.12	20.86	2.58	0.052	—	19.0
		CF 8 (SCS13A)		68	0.063	1.07	0.64	8.08	20.64	0.31	0.062	—	12.7
		CF 3 (SCS16A)	Centrifugal casting	P1	0.036	1.12	0.59	8.10	20.49	0.04	0.056	—	15.5
				P2	0.019	0.94	0.74	9.38	20.20	0.16	0.040	—	12.2
			Static casting	69	0.023	1.13	0.63	8.59	20.18	0.34	0.028	—	19.6

* : Ferrite content of base metal was calculated by ASTM A800 (%)

1

2. TEST METHODS

The chemical compositions of the base metals are shown in Table 1[2,8,10]. The base metals are mainly centrifugal cast pipes (thickness is approximately 70 mm) of CPF8M (hereinafter referred to as CF8M) (SCS14A) having ferrite contents of approximately 10 to 26% (calculated by ASTM A800), and the rest were CPF8 (hereinafter referred to as CF8) (SCS13A) or the equivalent not containing Mo. The plate thickness of the static casting is approximately 140 mm. The table 1 shows materials used in the other studies[2,10]. For the calculation of the ferrite contents (F%) in the base metals, the following equation obtained from the drawing of ASTM A800 by multiple regression analysis was used.

$$F\%(\%) = -4.834366 - 56.80472X + 134.641X^2$$
$$- 99.90123X^3 + 30.02316X^4 \quad \cdots\cdots (1)$$

$$X = Creq/Nieq$$

$$Creq = Cr + 1.5 \times Si + 1.4 \times Mo + Nb - 4.99$$

$$Nieq = Ni + 30 \times C + 0.5 \times Mn + 26 \times (N - 0.02) + 2.77$$

Where C, Si, Mn, Cr, Mo, Ni, Mo, Nb are in wt.%

The test materials were heated at the aging temperatures of 300, 350, 400, and 450°C for up to 40,000 hours, and the following tests were carried out. For the tensile tests, round bar tensile test specimens of 10 mm in diameter were used. The tests were carried out at room temperature and 325°C in accordance with ASTM A370 and ASTM E8. For the impact tests, Charpy impact test specimens of 10mm thickness with 2mm V-notch were used. These tests were also carried out at room temperature and 325°C in accordance with ASTM A370 and ASTM E23. For the fracture toughness tests, ITCT test specimens as described in ASTM E813-85 were used. The tests were carried out in accordance with ASTM E813-89.

In this study, J_Q is expressed as J_{Ic} even if it is invalid. The fracture toughness values with a stable crack extention Δa of 6 mm were obtained from the J-Δa curve, and expressed as J_6.

3. AGING PARAMETER

The degree of embrittlement can be obtained using the Arrhenius extrapolation of test data at higher temperature. The aging time to reach a given degree of embrittlement at different temperatures can be determined from the following equation[6].

$$P = Log_{10}(t) + 0.4343 \frac{Q}{R} \left(\frac{1}{673.2} - \frac{1}{T} \right) \quad \cdots\cdots (2)$$

where Q is the activation energy (100 kJ/mol), T is the aging temperature (K), t is the aging time (hours), R is the gas constant (0.008368 kJ/mol.K), and P is the aging parameter.

4. EXPERIMENTAL RESULTS

4.1 Tensile Properties

Fig. 1 shows examples of the changes of the 0.2% proof stress and tensile strength for the base metal aged at 300, 350, 400°C.

It is recognized that the tensile strength tends to increase with aging time, but the 0.2% proof stress does not seem to change. This tensile strength increasing tendency grows with increasing aging temperature. The reason why the proof stress is not affected by thermal aging is considered to be that tensile strain occurs mainly in the austenite phase up to the 0.2% proof stress. Namely, it is considered that hardening due to thermal aging occurs mainly in the ferrite phase, and austenite phase is not changed by aging.

Using these data, as described below, the true stress-strain curve prediction model after long term aging was studied.
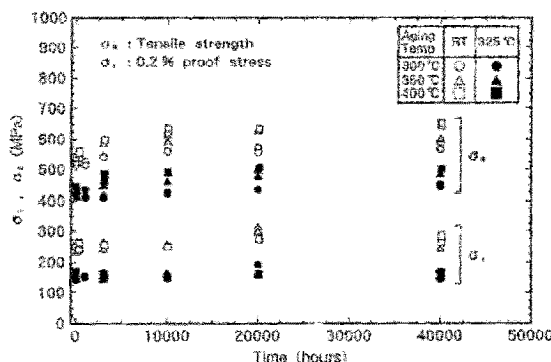

Fig. 1 Effect of Aging on Tensile Properties (No. A-A, CF8M, F%=10.3%)

4.2 Charpy Impact Test Properties

Fig. 2[6] shows the change in the Charpy absorbed energy (at 325°C) due to aging for the base metals aged at 300, 350, and 400°C. The Charpy absorbed energy reduces more with increasing aging temperature. In addition, the higher the ferrite content is, the lower the toughness after aging becomes.
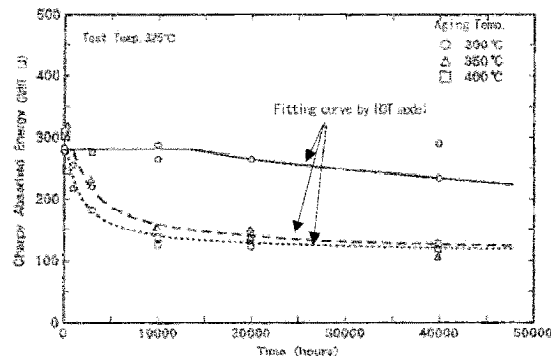

Fig. 2 Effect of Aging Time on Charpy Absorbed Energy (No. A-A, CF8M, F%=10.3%)

The change in the toughness of all materials tends to saturate after heating at 400°C for 20,000 to 40,000 hours. In this figure, the fitting curve by the toughness prediction model (H3T) mentioned below is also shown.

4.3 Fracture Toughness Properties

Fig. 3[6] shows the J-Δa curves of the base metal (A-A material) with aging at 400°C. The slope of the J-Δa curve
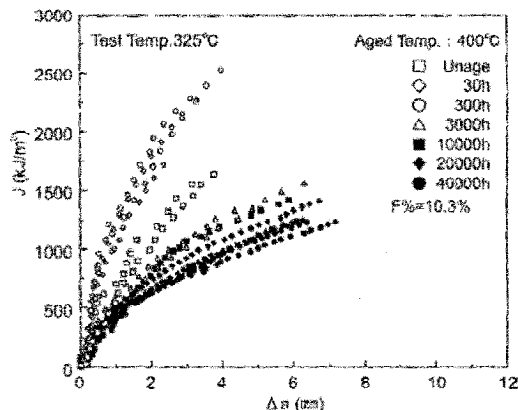

Fig. 3 J-Δa curve (Aging Temp. : 400°C, No. A-A, F%=10.3%)

2

tends to reduce as aging progresses. The J_{Ic} change due to thermal aging shows a tendency similar to that of the Charpy absorbed energy, and tends to decrease more with increasing aging temperature.

The aging parameters arranged with respect to J_6 (J integral value at $\Delta a=6$ mm) are shown in Fig. 4. Aging data for temperatures in the range of 300 to 450°C are well correlated with the aging parameters P.

4.4 Transmission Electron Microscopy

Transmission electron microscopy (TEM) analysis was carried out.

Two basic features of the ferrite phase sub-structure were identified by the TEM analysis of thin foils in aged material. The first, is the so-called mottled image (α ' phase), typically with contrast variations and the second, the presence of a G-phase, homogeneously distributed in ferrite for the material aged at 450°C for 3,000 and 10,000 hours[9].

The profiles of concentration of Fe and Cr in the ferrite phase have been investigated for CF8M by APFIM before and after aging. It was recognized that the amplification of Cr concentration of ferrite phase after the thermal aging was larger than that for unaged material and their ferrite phases are separated.
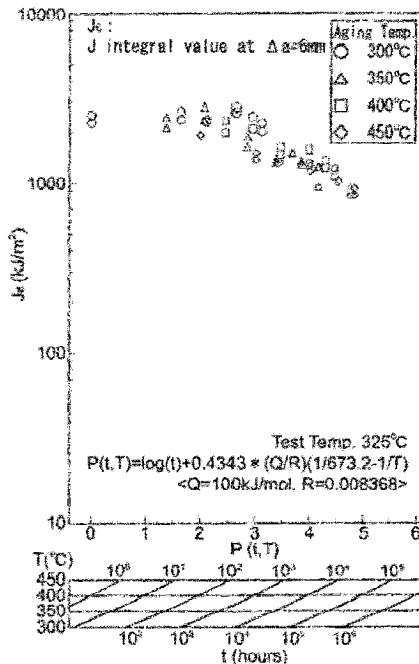

Fig. 4 J_6 and Aging Parameter P (No. A-A, F%=10.3%)

Fig. 5[9] shows the illustration for the mechanism of thermal aging embrittlement in duplex stainless steels. Before thermal aging, the Cr concentration of the ferrite phase is approximately 25%. However, the ferrite phase is separated into the α ' phase (Cr rich phase) with a Cr concentration of 70 to 80% and the α phase (Fe rich phase) with a small Cr concentration and a high Fe concentration by the thermal aging. Therefore, it is clear that thermal aging embrittlement is mainly caused by the phase separation (spinodal decomposition).

5. DEVELOPMENT OF PREDICTION MODELS

5.1 Prediction Method of True Stress-True Strain Curve (TSS Model)

Based on aging tests for predicting the stress- strain curve after thermal aging, we have developed a prediction method
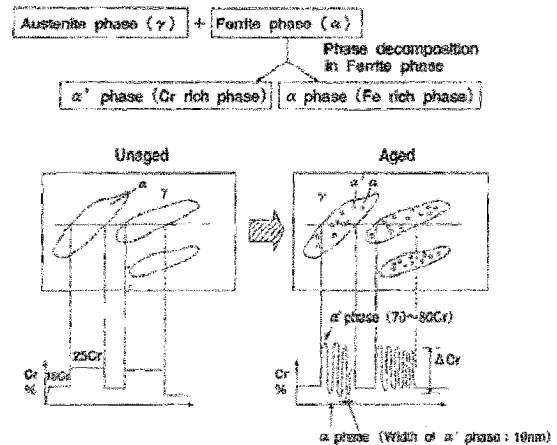

Fig. 5   Mechanism of Thermal Aging Embrittlement for Cast Duplex Stainless Steels

(TSS model: True Stress-True Strain model). For the development of this model, the results of the tension tests of the base metals aged at aging temperatures of 300, 350, and 400°C for up to 40,000 hours in this study[8] were used.

The stress-strain data at 325°C obtained by the aging tests were applied to the Ramberg-Osgood stress-strain equation shown below, and n and α were obtained.

$$\frac{\varepsilon}{\varepsilon_y} = \frac{\sigma}{\sigma_y} + \alpha \left(\frac{\sigma}{\sigma_y} \right)^n \qquad (3)$$

where σ is true stress (MPa) ; ε is true strain ; σ_y is 0.2% proof stress ; and ε_y is σ_y/E ; α is α, constant ; n is an exponent, E is Young's modulus (174000MPa at 325°C.)

The relationship between each of the 0.2% proof stress (σ_{y0}) and flow stress (σ_{f0}) of unaged material and chemical composition (ferrite content, C, etc.) was obtained using multiple regression analysis. Analysis for σ_{f0} is shown in Fig. 6.
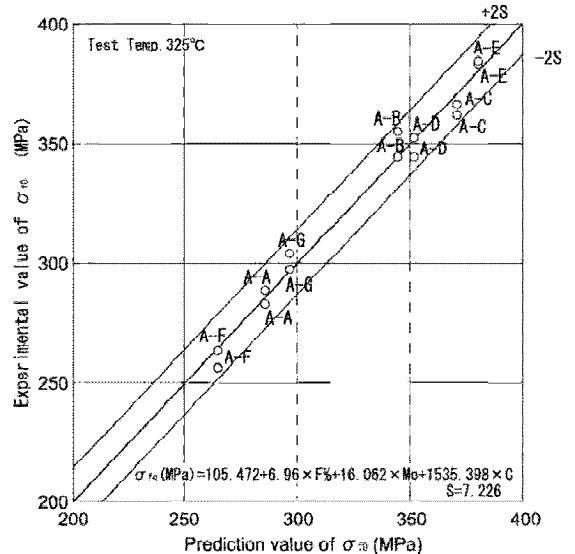

Fig. 6   Comparison of Experimental Values and Prediction Values for Unaged Flow Stress σ_{f0}

Next, in order to know a change in σ_y and σ_f after thermal aging, the ratios of σ_y / σ_{yo} and σ_f / σ_{fo} after thermal aging are obtained in relation to the aging parameters as shown for σ_f in Fig. 7. Based on the relationship of σ_f after thermal aging thus obtained, n and α after thermal aging can be obtained as shown in Fig. 8 (F%<23%). The prediction equations thus set are shown in Table 2. Using the prediction equations of n, α, σ_y, and σ_f, the true stress-true strain curve after thermal aging can be predicted from the chemical composition. The predicting procedure in the true stress-true strain curve prediction method after thermal aging is shown in Fig. 9.

Table 2   True Stress-Strain Prediction Equations (TSS model,Temp:325℃)

		Prediction equation (unaged)	S	eq.
Unaged σ_{yo} (MPa)		0.2% proof stress : σ_{yo}=6.653+5.385×F%+10.007×Mo+1535.385×C	9.450	(a)
Unaged σ_{fo} (MPa)		Flow stress : σ_{fo}=105.472+6.96×F%+16.062×Mo+1535.398×C F% : Ferrite Content (%) calculated by ASTM A800 Mo, C : CMTR (wt%)	7.226	(b)

	F%	Prediction equation (after aging)	S	note	eq.
σ_y / σ_{yo} -P(t,T)	F%<23%	Y=(1+1.071)/2-(1-1.071)/2× tanh((X-1.617)/0.916)	0.069	Y= σ_y / σ_{yo} X=P(t,T)	(c)
	F%≧23%	Y=(1+1.144)/2-(1-1.144)/2× tanh((X-3.020)/1.462)	0.053		(d)
σ_f / σ_{fo} -P(t,T)	F%<23%	Y=(1+1.161)/2-(1-1.161)/2× tanh((X-2.996)/0.929)	0.051	Y= σ_f / σ_{fo} X=P(t,T)	(e)
	F%≧23%	Y=(1+1.247)/2-(1-1.247)/2× tanh((X-3.148)/0.919)	0.039		(f)
n- σ_f (MPa)	F%<23%	Y = X × (-0.005)+(6.763)	0.552	Y=n X= σ_f	(g)
	F%≧23%	Y = X × (-0.011)+(9.734)	0.484		(h)
α- σ_f (MPa)	F%<23%	Y = X × (-0.011)+(6.054)	0.577	Y= α X= σ_f	(i)
	F%≧23%	Y = X × (-0.013)+(7.305)	0.347		(j)

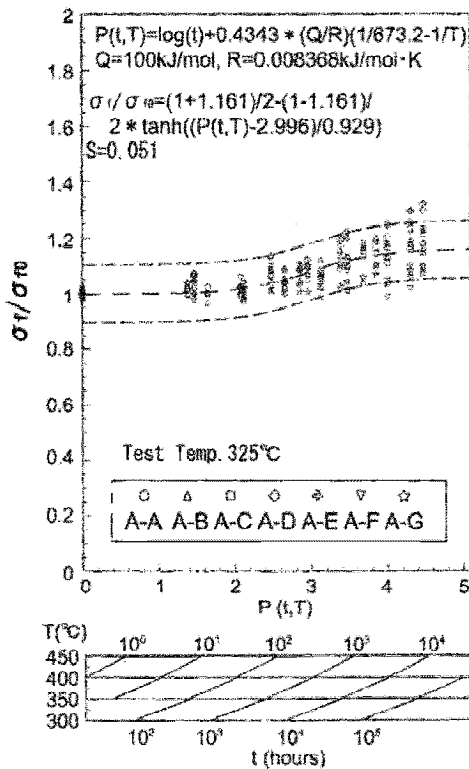note : P(t,T)=log(t)+0.4343·(Q/R)(1/673.2-1/T), T : K, t : hours, Q : 100kJ/mol, R : 0.008368kJ/mol·k

(F%<23%)

$n = \sigma_f \times (-0.005)+(6.763)$
$S=0.552$

(F%<23%)

$\alpha = \sigma_f \times (-0.011)+(6.054)$
$S=0.577$

Fig. 8   n, α and flow stress σ_f

$P(t,T)=\log(t)+0.4343 * (Q/R)(1/673.2-1/T)$
$Q=100kJ/mol, R=0.008368kJ/mol·K$

$\sigma_f / \sigma_{fo}=(1+1.161)/2-(1-1.161)/2 * \tanh((P(t,T)-2.996)/0.929)$
$S=0.051$

Test Temp. 325℃

○	△	□	◇	◆	▽	☆
A-A	A-B	A-C	A-D	A-E	A-F	A-G

Fig. 7   Ratio of Flow Stress (σ_f / σ_{fo}) Versus P(t,T), F%<23%
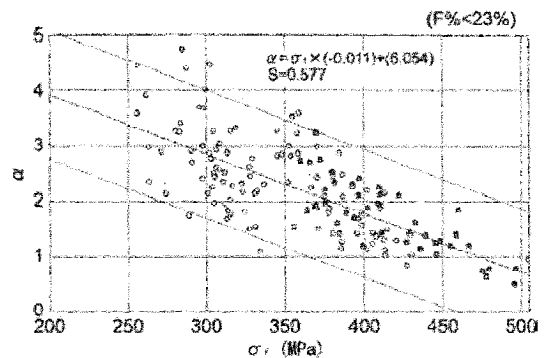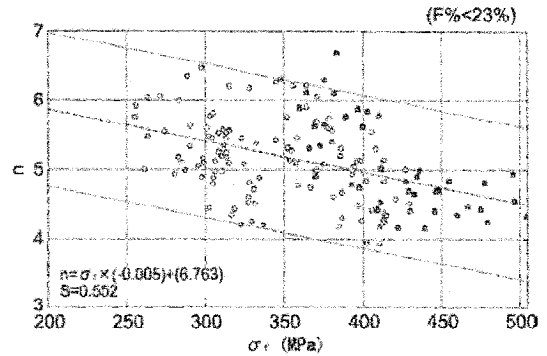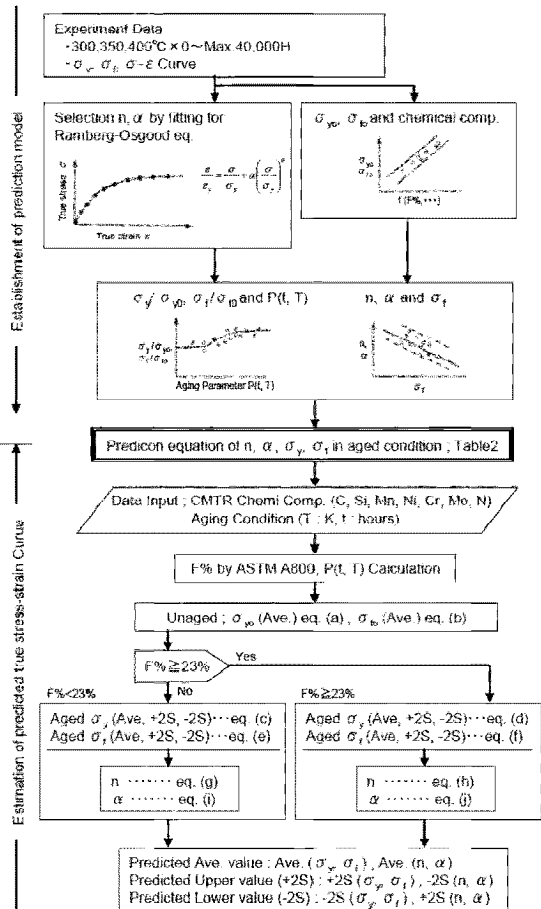
Fig. 9   Estimation Process of Predicted True Stain-Stress Curve (TSS model)

4

11

The experimental data and predicted true stress-true strain curve after thermal aging are shown in Fig. 10. The experimental data and predicted true stress the true strain curves are rather comparable with each other.
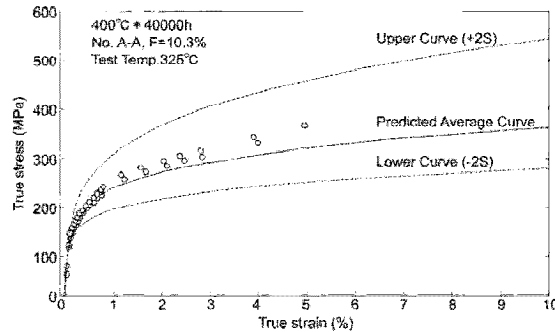

Fig. 10 Experimental Data and Predicted True Stress-True Strain Curve by TSS Model

5.2 Prediction Method of Fracture Toughness (H3T Model)

The toughness degradation prediction model has been developed on the basis of the H3T (Hyperbolic-Time-Temperature-Toughness) model. The H3T model expresses the relationship of the Charpy absorbed energy, J_{Ic}, and J_6 to the aging time with the following hyperbolic function as shown in Fig. 11[8,10]. Using the results[8] of this study and document data[2,10], the H3T model has been developed.

$$C_V, J_{Ic}, J_6 = A + \frac{B}{t + C} \quad \cdots\cdots (4)$$

where,

t : Aging time, hours
A : Fully aged toughness, kJ/m^2
B : Constant relating to aging temperature
C : Constant relating to aging time

Now it is assumed that $B = \exp(D/T + Co)$ and $D = Q/R$, where T is the aging temperature, Co is a constant, and R is the gas constant. When T is T_i, B is B_i. When $T = T_j$, B is B_j.

$$B_i / B_j = \exp[D(1/T_i - 1/T_j)] \quad \cdots\cdots (5)$$

$$B_i / B_j = \exp[(Q/R)(1/T_i - 1/T_j)] \quad \cdots\cdots (6)$$

The activation energy Q (kJ/mole) obtained from the temperature dependence of B is defined to be the embrittlement activation energy.

On the other hand, the initiation activation energy F is defined from the temperature dependence of the initiation time of tertiary embrittlement t_F, as shown in Fig. 11 namely

$$t_{F_i} / t_{F_j} = \exp[(F/R)(1/T_i - 1/T_j)] \quad \cdots\cdots (7)$$

From equation (4), the relational expression B at temperatures T_i and T_j is as shown below.

$$\frac{B_i}{t_{F_i} + C_i} = \frac{B_j}{t_{F_j} + C_j} \quad \cdots\cdots (8)$$

From equation (8), $t_{Fj} + C_j$ at T_j is determined using $t_{Fi} + C_i$ at T_i as shown below.

$$t_{F_j} + C_j = \frac{B_j}{B_i}\left(t_{F_i} + C_i\right) \quad \cdots\cdots (9)$$

Next, from equation (4), the equations of embrittlement prediction model at temperatures T_i and T_k is as shown below.

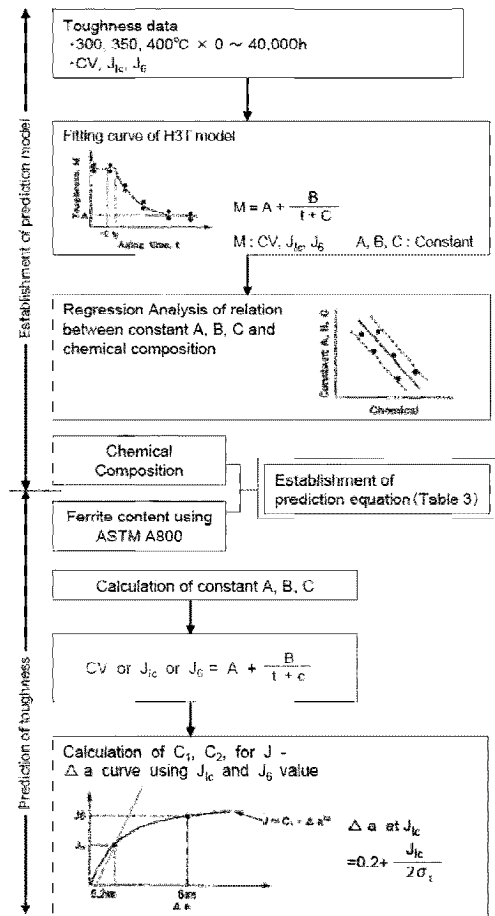$$M_i = A + \frac{B_i}{t + C_i} \quad \cdots\cdots (10)$$

Fig. 11 Flow Chart of The Toughness Prediction Model (H3T Model)

$$M_k = A + \frac{B_k}{t + C_k} \quad \cdots\cdots (11)$$

From these equations, the toughness M_k at any temperature T_k, can be calculated using a constant at T_i and Q and F as follows.

$$M_k = A + \frac{B_i \exp\left[\frac{Q}{R}(1/T_k - 1/T_i)\right]}{t \cdot \left(t_{F_i} + C_i\right)\exp\left[\frac{Q}{R}(1/T_k - 1/T_i)\right] \cdot t_{F_i}\exp\left[\frac{F}{R}(1/T_k - 1/T_i)\right]} \quad \cdots\cdots (12)$$

Fig. 11 shows the flow chart of the toughness prediction model. First, the data for the aging temperature of 400°C is fitted with the H3T model to obtain the constant A (the fully aged lowest toughness). With this constant A determined, the data for aging at 300 and 350°C are fitted with the H3T model to obtain the constant B and C at the aging temperatures of 300 and 350°C. By obtaining the relationship of the above constants A, B, and C to the chemical composition, the prediction expression can be obtained. Fig. 12 shows the relation of the constant A (after full aging) of J_{Ic} to the ferrite content.

Table 3[10] shows the H3T model for absorbed energy at room temperature and 325°C, fracture toughness at 325°C, the constant A of J_{Ic} and J_6 (the fully aged lowest toughness) obtained in the same manner when the operating temperature is 325°C. Fig. 13 shows the applicable flow chart for the H3T model.
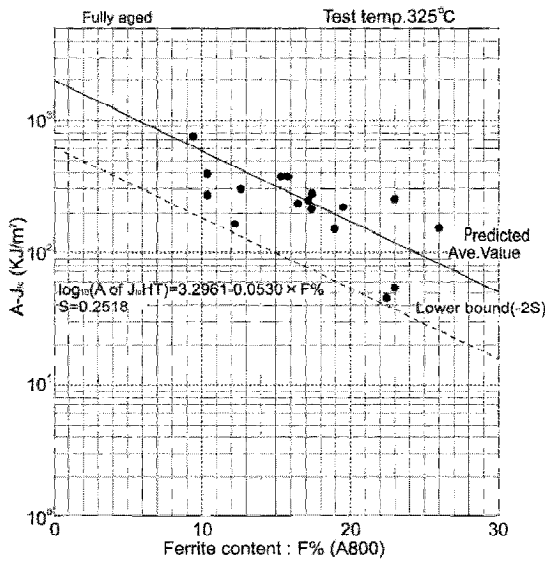
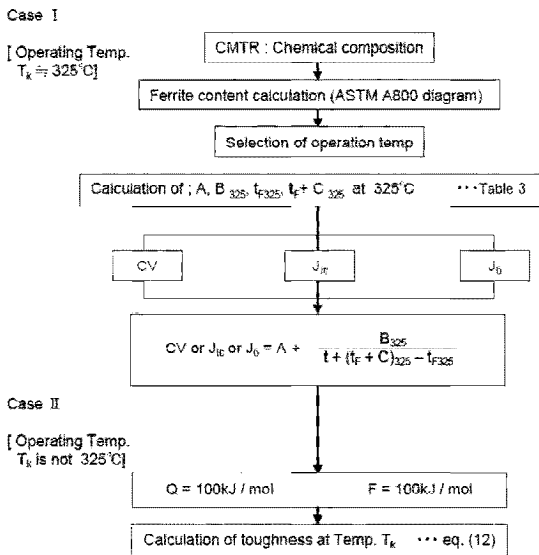**Fig. 12** Fully Aged Toughness Constant A of 325°C J_{Ic} versus F%

Fig. 13 Estimation Process of Toughness Prediction Model (H3T Model)

When the operating temperature is different from 325°C, the prediction model can be evaluated conservatively using the activation energy Q = 100 kJ/mole.

In evaluating the integrity of duplex stainless steels after thermal aging, fracture mechanics method may be used and, therefore, it is important to predict the J-Δa curve. When the J_{Ic} and J_6 values at an optional aging condition are obtained, the J-Δa curve can be obtained by the following equation with the H3T model by giving the flow stress as shown in Fig. 11, and the integrity can be evaluated.

$$J = C_1 \times \left(\Delta a\right)^{C2} \quad \cdots \cdots (13)$$

Fig. 14 shows predicted fracture toughness (J-Δa curves: average and -2S lower bound curve) for No. A-A material after fully aging.

The lower bound (dotted line) by the H3T model was found to have a conservative prediction accuracy.

Table 3 Constants of Fully Aged Toughness Prediction Model when the Operating Temperature is 325°C (H3T Model)

		Predicted equation	S
CV-RT (Charpy absorbed energy(J) at RT	A	Log_{10} (A of CV-RT)= 2.2818 -0.0472×F%	0.1411
	B_{325}	Log_{10} B_{325}= 6.0909 -0.2861×Mo	0.2621
	t_{F325}	Log_{10} t_{F325}= 19.7270 -0.4750×Cr +6.2846×Ni -13.9003×N	0.1124
	$(t_F+C)_{325}$	Log_{10} $(t_F+C)_{325}$= 3.9369 -0.3784×Mo	0.1597
CV-HT (Charpy absorbed energy at 325°C)	A	Log_{10} (A of CV-HT)= 2.8357 -0.0592×F%	0.1638
	B_{325}	Log_{10} B_{325}= 8.5909 +2.4273×Mn -0.4328×Ni	0.1606
	t_{F325}	Log_{10} t_{F325}= 22.8968 -2.0122×Mn -0.8227×Cr -23.0802×C	0.0743
	$(t_F+C)_{325}$	Log_{10} $(t_F+C)_{325}$= 4.9882 -0.4121×Mo	0.1454
J_{Ic}-HT (J_{Ic} at 325°C, kJ/m²)	A	Log_{10} (A of J_{Ic}-HT)= 3.2961 -0.0530×F%	0.2518
	B_{325}	Log_{10} B_{325}= 5.7869 +0.9256×Mn	0.1514
	t_{F325}	Log_{10} t_{F325}= 4.3047 -19.1095×N	0.2732
	$(t_F+C)_{325}$	Log_{10} $(t_F+C)_{325}$= 1.5354 +0.2062×Ni	0.1417
J_6-HT (J_6 at 325°C, kJ/m²) J_6:J value at Δa 6mm	A	Log_{10} (A of J_6-HT)= 3.6699 -0.0490×F%	0.1490
	B_{325}	Log_{10} B_{325}= -1.7907 +0.4436×Cr	0.1783
	t_{F325}	Log_{10} t_{F325}= 7.6362 -0.3670×Ni -16.108×N	0.0892
	$(t_F+C)_{325}$	Log_{10} $(t_F+C)_{325}$= -2.9645 +0.3438×Cr -0.1648×Mo	0.0702

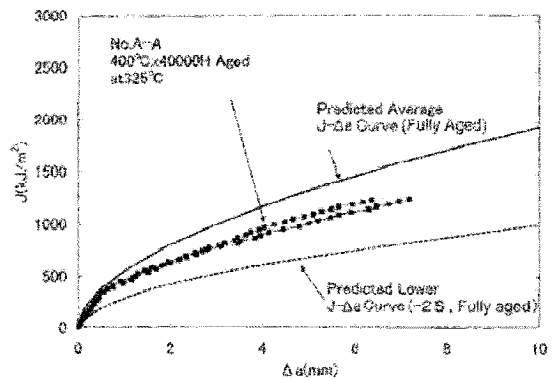note) F% : Ferrite content(%) by ASTM A800 diagram. C, Si, Mn, Cr, Ni, Mo, N (wt%)

Fig. 14 Predicted J-Δa Curve for Fully Aged Toughness (No. A-A, 400°C×40000H)

6. SUMMARY AND CONCLUSIONS

The mechanical tests were carried out for cast duplex stainless steels (CF8M, CF8) aged up to 40,000 hours. The results obtained can be summarized as follows.

(1) The Charpy absorbed energy and fracture toughness are lowered and tensile strength is increased with aging time. From the results of the electron microscopy and the APFIM analysis, the thermal aging embrittlement was verified to be caused by phase separation in the ferrite phase.

(2) Using the aging data up to 40,000 hours, the tensile properties (true stress-true strain curve) prediction method (TSS model) for long term aging was developed.

6

(3) In the same manner, the fracture toughness J_{Ic}, J_6, J-Δa curve prediction method (H3T model) for long term aging was developed.

ACKNOWLEDGEMENTS

REFERENCES

1. O.K. Chopra, et al., "Effects of Low-Temperature Aging on the Mechanical Properties of Cast Stainless Steels", Proceedings of the Winter Annual Meetings of ASME, Boston, MA., December 13-18, 1987.

2. O.K. Chopra, "Long-term embrittlement of cast duplex stainless steels in LWR Systems", NUREG/CR-4744 Vol.6, No.1, ANL-91/22, R5, August, 1992.

3. O.K. Chopra, et al., "Evaluation of aging degradation of structural components", in Proceedings of the Aging Research Information Conference, NUREG/CP-0122, Vol.2, 1992, pp396-386.

4. O.K. Chopra, et al., "Assessment of Thermal Embrittlement of Cast Stainless Steels", NUREG/CR-6177 ANL-94/2, May, 1994.

5. O.K. Chopra, "Thermal Aging of Cast Stainless Steels in LWR Systems : Estimation of mechanical properties" ASME PVP 1992.

6. W.Gysel, et al., "Influence of long-time aging of CF8 and CF8M cast steel at temperatures between 300 and 500°C on impact toughness and structual properties", ASTM STP 756, 1982, pp165-198.

7. S.Kawaguchi, et al., "The phase decomposition by thermal aging in duplex stainless steels", IIW DOC. IX-1747-94, September, 1994.

8. T.Tanaka, S.Kawaguchi, N.Sakamoto, K.Koyama "Thermal Aging of Cast Duplex Stainless Steels", ASME/JSME PVP, 1995.

9. S.Kawaguchi, N.Sakamoto, G.Takano, F.Matsuda, L.Mraz "Microstructual Changes and Fracture Behavior of CF8M Duplex Stainless Steels after Long Term Aging", Nuclear Engineering and Design 174, 1997. p273-285.

10. I.Suzuki, S.Kawaguchi, M.Koyama, H.Mimaki, M.Akiyama, T.Okubo, Y.Mishima, T.R.Mager "Long Term Thermal Aging of Cast Duplex Stainless Steels" The International Conference on Nuclear Engineering (ICONE-4), March, 1996.

11. A.Kirihigasi, S.Kawaguchi, S.Shimizu, Y.Fujioka, K.Sakai "NDT of Aged Duplex Stainless Steel using Mössbauer Spectroscopy" 14th International Conference on NDE in the Nuclear and Pressure Vessel Industries, Stockholm, Sep., 1996.

12. K.Hojo, I.Muroya, K.Koyama S.Kawaguchi, "Application of the Two-Criteria Approach to the Austenitic Cast Stainless Steel Pipe", The 5th International Conference of Nuclear Engineering (ICONE-5), May, 1997.

14

補足

図３中に示すＨ３Ｔモデル平均線及び下限線は、文献[1]に記載の予測モデルに当該材料の材料証明書より表２に示す諸条件をインプットして求めた予測線である。

具体的には文献[1]に従い、以下の式の係数をそれぞれ算出し予測線を作図する。

$$J_6 = A + \frac{B\exp\left[\frac{Q}{R}\left(1/T_k - 1/T_i\right)\right]}{t + (t_F + C)\exp\left[\frac{Q}{R}\left(1/T_k - 1/T_i\right)\right] - t_F\exp\left[\frac{F}{R}\left(1/T_k - 1/T_i\right)\right]}$$

ここで、上式の係数は以下である。

Q = 100 kJ/mol、

F = 100 kJ/mol、

R = 0.008368 kJ/mol K、

T_i = 598.2 K (= 325+273.2 ℃)、

T_k = 運転温度(時効温度) [K]であり、

　　　　H/L エルボ材 : T_k = 598.2 K (= 325+273.2 ℃)、

　　　　CO/L エルボ材 : T_k = 563.2 K (= 290+273.2 ℃)、

A、B、$t_F + C$ 及び t_F は平均線及び下限線に対して、

平均線 :

　　$\text{Log}_{10}\, A$ = 3.6699 - 0.0490×$F\%$

　　$\text{Log}_{10}\, B$ = -1.7907 + 0.4130×Cr

　　$\text{Log}_{10}\, t_F$ = 7.6362 - 0.3670×Ni - 16.108×N

　　$\text{Log}_{10}(t_F + C)$ = -2.9645 + 0.3438×Cr - 0.1648×Mo

下限線 (標準偏差 S の 2×S を考慮) :

　　$\text{Log}_{10}\, A$ = 3.6699 - 0.0490×$F\%$ - 2×0.1490

　　$\text{Log}_{10}\, B$ = -1.7907 + 0.4130×Cr - 2×0.1783

　　$\text{Log}_{10}\, t_F$ = 7.6362 - 0.3670×Ni - 16.108×N - 2×0.0892

　　$\text{Log}_{10}(t_F + C)$ = -2.9645 + 0.3438×Cr - 0.1648×Mo + 2×0.0702

である。